Geomechanics and Engineering, *Vol. 36, No. 1 (2024) 9-18*
https://doi.org/10.12989/gae.2024.36.1.009

Disintegration process and micro mechanism of mudstone under dry-wet cycles

Ji Chen[1,2,3], Ruyu Huang[4], Xinyu Luo[1], Xin Liao*[3] and Qiang Tang**[1,2,3]

[1]*School of Rail Transportation, Soochow University, Suzhou, 215131, China*
[2]*Graduate School of Global Environmental Studies, Kyoto University, Sakyo-ku, Kyoto 606-8501, Japan*
[3]*Faculty of Geosciences and Environmental Engineering, Southwest Jiaotong University, Chengdu 611756, China*
[4]*Human Resources and Social Security Bureau, Tonggu County, 336299, China*

(*Received January 24, 2022, Revised November 22, 2023, Accepted November 28, 2023*)

Abstract. With the rapid development of highways and railways, series of traffic safety issues emerged because of mudstone disintegration. To research on the mechanism and further guarantee the stability and safety of transportation infrastructure built on or near mudstone formations, the mudstone disintegration test of mudstone was carried out based on mudstone and sandy mudstone. The element types, cementation characteristics and pore characteristics of the tested specimens were studied by means of Scanning Electron Microscopy (SEM), X-ray Diffraction (XRD) and Image Pro Plus (IPP). The disintegration index of mudstone was approximately 1%, and even some specimens were difficult to be calculated, while the disintegration index of sandy mudstone is approximately 8.7%. According to the results, the two mudstones belong to grade II and III disintegration respectively, of which the sandy stone presents more extensive disintegration than mudstone. This phenomenon was distinguished that, the clay minerals of mudstone are approximately 25% more abundant than those of sandy mudstone, and the unit pore area is 20 μm^2 larger, which result in different microstructure and water absorption capacities. In the liquid phase, the ions in the mudstone specimens were exchanged and combined with water molecules in the environment during the whole disintegration process. This results in continuous spalling and fragmentation of clay minerals, the emergence of secondary fractures, and the deepening of primary fractures.

Keywords: disintegration test; dry-wet cycle; microstructure; mineral composition; mudstone

1. Introduction

Mudstone is a strongly consolidated rock formed by a certain degree of epigenesis, such as extrusion, dehydration, recrystallization, and cementation (Koralegedara and Maynard 2017). Mudstones are widely distributed throughout the world but cause many engineering problems (Milroy *et al.* 2019).

Therefore, the physical and mechanical properties, water absorption capacity and disintegration characteristics of mudstone have been studied extensively.

The physical and mechanical properties of mudstone are affected by many factors, such as mineral composition, clay minerals percentage and porosity. Through the triaxial test of mudstone soaked at different time, the influence of different degree of water-rock interaction on the fracture mechanical properties of mudstone was studied (Lian *et al.* 2020, Sargent *et al.* 2016). The experimental results show that the fracture mechanical behavior of natural mudstone is significantly affected by water-rock interaction, and its peak load decreases with increasing soaking time. In some studies, Scanning Electron Microscopy (SEM) and molecular dynamics simulation were studied and conclude that water absorption and clay minerals' expansion were the main causes of disintegration in mudstone (Iyare *et al.* 2021, Dner *et al.* 2021, Gautam and Shakoor 2013). Aside from the influence of water and clay minerals, the temperature is another significant factor. Mechanical tests based on varying temperature were conducted and the stress-strain curve of mudstone revealed that the elastic modulus and peak strength of mudstone first increased and then decreased with increasing temperature (Sakai and Nakano 2015).

More research focuses on the influence of the water absorption of mudstone on its degradation characteristics. The mudstone water absorption process includes decelerating water absorption and constant water absorption (Kévin *et al.* 2020). Some studies have used the Nuclear Magnetic Resonance (NMR) tests to study the development of cracks in mudstone after encountering water. It is concluded that with increasing soaking time, the pore size in the fractured mudstone becomes larger and eventually penetrates, and the strength of the rock decreases continuously (DeReuil *et al.* 2019, Shakoor and Gautam 2015, Kim *et al.* 2018). Subsequently, liquid water absorption experiments were carried out on mudstone specimens of different lithologies under the condition of no water pressure, and the function of water absorption over time in the whole process was obtained (Meisels *et al.* 2015). Through X-ray diffraction (XRD), SEM and Mercury Intrusion Porosimetry (MIP), the results show that

*Corresponding author, Associate Professor
E-mail: xinliao@swjtu.edu.cn
**Professor
E-mail: tangqiang@suda.edu.cn

ISSN: 2005-307X (Print), 2092-6219 (Online)

Table 1 Main minerals of mudstone specimens

Specimen number	Quartz (%)	Clay minerals (%)				Other Minerals (%)
		Montmorillonite	Illite	Chlorite	Kaolinite	
N-6	29		29	11	9	16
N-19	25		28	6	9	26
N-28	54		10	4	4	22
N-46	41	6	20	9	9	15
N-54	41		20	9	6	18
N-56	52		10	6	4	22
N-62	52		11	6	4	21

the main factor affecting the water absorption of mudstone is not the clay mineral content, but the micropores. Microstructural and morphological changes of mudstones after water absorption were studied and analyzed through XRD and SEM method based on microstructure, deformation characteristics and energy analysis theories. This research revealed the correlation clay mineral content, pore area and water absorption and deformation of mudstone (Feng *et al.* 2022). Through an experimental study on the water absorption process of different hydro-chemical solutions, the influence of different solution properties on the law of water absorption of mudstone is analyzed (Tang *et al.* 2014, Tang *et al*. 2015,). The order of influence is pH value, main clay mineral type, compactness, clay mineral content and solution ion concentration (Gautam and Shakoor 2016, Tang *et al*. 2017).

In regard to the water absorption properties of mudstone, it must be inseparable from its disintegration deformation characteristics. It mainly includes the rule and mechanism of disintegration, and the purpose is to reduce the influence of the disintegration and deformation behavior of mudstone on actual engineering. The disintegration and softening of mudstone are the macroscopic reflection of the internal structure and crack changes of mudstone (Arman *et al.* 2021, Mori *et al.* 2018, Tang *et al.* 2018). The disintegration characteristics of red-bed mudstone are most affected by the sedimentary environment, and the correlation between disintegration characteristics and fractal characteristic parameters is relatively high (Selen *et al.* 2019, Vu *et al.* 2019, Aksoy *et al.* 2019). The hydraulic instability of red bed soft rock is mainly caused by illite. There are also some experiments on red layered mudstone, and the results show that weathering disintegration is carried out from the surface to the interior under the action of external forces, and the surface mudstone continues to disintegrate and fall off (Pesce *et al.* 2020, Park *et al*. 2016). The disintegration is mainly concentrated within 10 cm from the surface, and the disintegration rate is mainly affected by the external ambient temperature and rainfall.

Influenced by the external environment, mudstone easily shows the characteristics of water absorption disintegration and strength decline, resulting in many engineering problems, such as common slope landslides, roadbed settlement, and mine collapse (Momeni *et al.* 2017). How the microscopic level of mudstone changes in the process of disintegration needs to be further studied. Therefore, this paper mainly utilized mudstone and sandy mudstone as the research objects for the characteristics of water-absorption disintegration and the microscopic transformations throughout the dry-wet cycle process. This paper was a coupled research based on the disintegration test and micro mechanism, in an effort to distinguish the main factors of disintegration and provide theoretical basis for the implementation of future research.

2 Materials and methods

2.1 Materials

In this study, a region in Xining, China, was as the main study area. There is abundant groundwater, which has a great impact on the engineering properties of rocks and poses a great potential risk to the safety of nearby construction (Dupontnivet *et al.* 2008). According to the field survey, the mudstone outcrops in the study area include the Cretaceous strata of Mesozoic and the Neoproterozoic strata of Cenozoic (Chen *et al*. 2022). Among them, the Neoproterozoic mudstone is the most extensive. The structure of the Cretaceous mudstone is stable, the structure of the Neoproterozoic mudstone is poor, and the disintegration phenomenon is more obvious after encountering water. In this study, both mudstones were selected (Yin *et al.* 2017).

Specimens with relatively complete structures and good overall shapes were selected for the test. Specimens were taken in the experimental area and brought back to the laboratory under seal. The specimens before water absorption were dark gray, dark purplish red, compact structure and obvious bedding. Retrieved specimens were numbered according to formation and sampling order. The specimen numbers were N-6, N-19, N-28, N-46, N-54, N-56 and N-62. XRD was used to determine the characteristics of the test pores, and the test results are shown in Table 1. Other than high percentage of Quartz and Clay minerals, different specimens contain varying percentage of other minerals such as feldspar, calcite, dolomite, siderite and zeolite, with the total proportion from 15% to 26%.

Based on the data presented in Table 1, it is evident that Cretaceous mudstone in Xining exhibits a substantial content of clay minerals. This notable presence of clay minerals raises the possibility of influencing the water

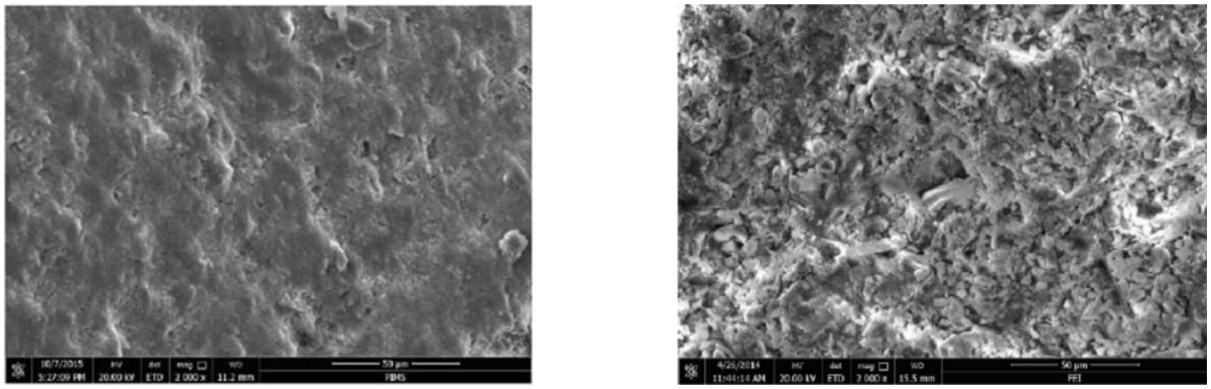

(a) Flat sheet mudstone (b) Clastic granular mudstone

Fig. 1 SEM images of mudstone specimens

absorption characteristics of the specimens under investigation. The water absorption properties of mudstone are intricately linked to its structural composition. In light of this, our study delves into a detailed analysis of the microstructure of the mudstone specimens, focusing specifically on two key aspects: Unit type and Pore characteristics, in effort to provide a comprehensive understanding of how the microstructural features, particularly unit type and pore characteristics, contribute to the water absorption behavior of the mudstone specimens.

2.1.1 Unit type

The material basis of the microstructure of the mudstone is mainly the clay thin layer structure formed by the clay mineral particles in a certain arrangement, or the clay thin layers are stacked together into a thin layer stacking structure. These thin layers have strong properties of water absorption expansion and water loss shrinkage. SEM was applied to observe the mudstone specimen, and the SEM images are shown in Fig. 1.

From the analysis of SEM images, the mudstone specimens are divided into two main categories according to the characteristics of the units: flat stratified stromatolites are the main units, as shown in Fig. 1(a), which belong to mudstone. The second is mudstone dominated by clastic grain units, as shown in Fig. 1(b), which belongs to sandy mudstone (Chen *et al.* 2013). According to SEM image analysis, N-6, N-19, N-46 and N-54 are mudstones, while N-28, N-56 and N-62 are sandy mudstones.

2.1.2 Pore characteristics

Pore refers to the space in rock that is not filled by clastic particles, cementing materials or other materials. Pore structure refers to the geometric shape, size distribution characteristics and connection relations of pores and throats in rock. Table 2 shows the pore characteristics measured with MIP for some representative specimens.

In Table 2, N-46 and N-54 belong to mudstone, while N-56 and N-62 belong to sandy mudstone. It can be concluded from the table that the plane porosity of mudstone in the Xining area is between 0.07% and 0.3%, and the plane porosity is low. This is because the mudstone in Xining, China, is buried deeply, and the pores are squeezed under the action of gravity. The plane porosities of mudstone N-46 and N-54 are obviously smaller than those of mudstone N-56 and N-62, which is related to the microstructure. There are more clastic grain units in sandy mudstone, which is also related to its formation environment. The formation environment of sandy mudstone is relatively unstable, which leads to this difference.

Table 2 Pore structure parameters of specimens

Specimen Number	Plane porosity (%)	Average pore size (μm)	Circularity	Fractal dimension
N-46	0.10	1.94	3.98	1.15
N-54	0.07	2.48	1.65	1.13
N-56	0.20	2.77	1.78	1.10
N-62	0.30	2.04	1.59	1.09

2.2 Disintegration test

The mudstone disintegration test can be divided into two simultaneous parts: specimen disintegration and surface detection. The disintegration test shall be performed as follows. First, the quality of the specimens in the dry state was weighed. Before the dry-wet cycles, the mudstone specimens were first put into a cylindrical sieve cylinder of a TX255/NBJSY - 1 disintegrating test apparatus. The sieve cylinder with the specimens was put into the water tank and injected with distilled water at 20°C ± 2°C. The soaking water level should be approximately 20 mm below the axis of rotation. The sieve barrel was rotated at a speed of 20 r/min for 10 min, and then placed in an oven at 105°C - 110°C for 24 h drying. They were cooled to room temperature and weighed. The above is one cycle, and a total of five cycles would be carried out (Luo *et al.* 2021).

The steps of specimen surface observation during the disintegration process are as follows. The specimens were put into the beaker immersed with water, and the electron microscope was adjusted vertically to capture the whole picture of the specimen accurately. Automatic photographing was set every 10 min. The phenomenon of disintegration was detected and recorded throughout the whole disintegration test.

In this study, the disintegration index I_d is used to

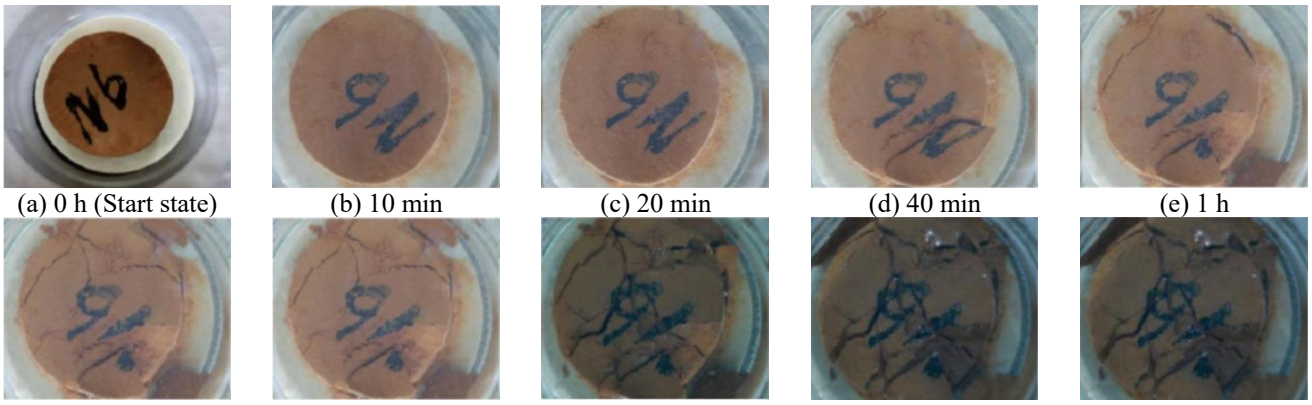

(a) 0 h (Start state) (b) 10 min (c) 20 min (d) 40 min (e) 1 h
(f) 1 h 30 min (g) 2 h 20 min (h) 4 h 20 min (i) 6 h 50 min (j) 2 d (Final state)

Fig. 2 Disintegration process of N-56

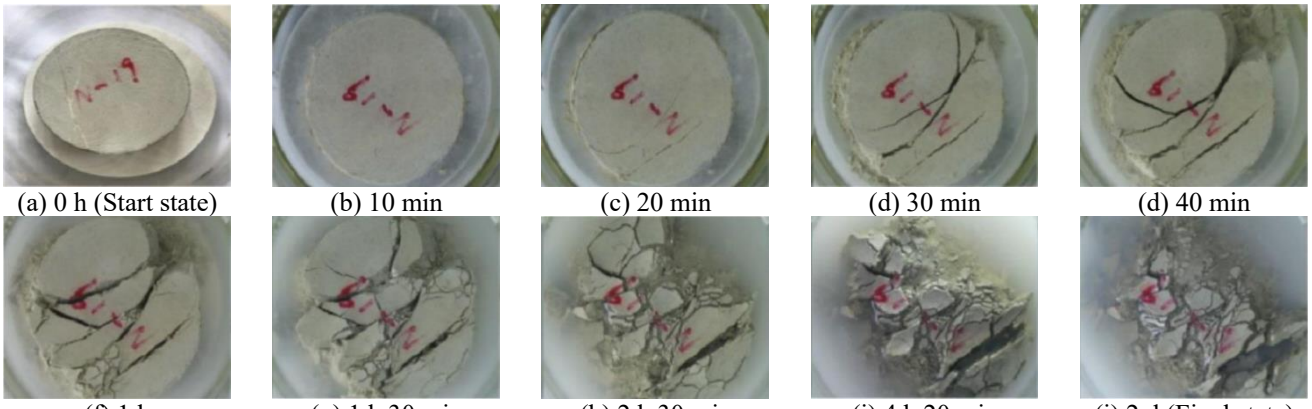

(a) 0 h (Start state) (b) 10 min (c) 20 min (d) 30 min (d) 40 min
(f) 1 h (g) 1 h 30 min (h) 2 h 30 min (i) 4 h 20 min (j) 2 d (Final state)

Fig. 3 Disintegration process of N-19

quantify the disintegration process of mudstone specimens. The I_d is defined as the percentage of the mass of the specimen with grain size greater than 2 mm in the total mass of the original specimen after two dry-wet cycles (ASTM D4644-08). The specific formula is Eq. (1)

$$I_d = \frac{M_{r>2}}{M} \times 100\% \quad (1)$$

In this formula, $M_{r>2}$ is the total mass of the part of the mudstone specimen larger than 2 mm after two dry-wet cycles and M is the total mass of the mudstone specimen.

3. Results and discussion

3.1 Disintegration test of mudstone

In the disintegration experiment, the disintegration characteristics of mudstone specimens N-6, N-19, N-28, N-46 and N-56 are more regular and representative. The following is mainly to analyze the disintegration characteristics of these specimens. Among them, N-6, N-19 and N-46 belong to mudstone, and N-28 and N-56 belong to sandy mudstone. The disintegration process of each specimen is as follows.

The initial color of rock specimen N-6 is earthen yellow, and there are some darker parts on the side. As shown in Fig. 2, powder on the surface of the specimen will fall off after water is added. Twenty minutes later, fine cracks appeared and gradually extended in the following time. An hour later, collapse appeared around the specimen, and the side cracks gradually became dense. After 1 h 30 min, several slender and connected cracks were formed on the surface of the specimen, expanding continuously. When the cracks deepen to a certain extent, the specimen collapses into several pieces. After 6 h, the variations of rock specimen become very slow and basically tends to be stable.

The initial color of the N-19 rock specimen is gray, and the surface is smooth with fine cracks on the surface and sides. As shown in Fig. 3, a slender crack appeared after the specimen was immersed in water for 10 min. Within 1 h, the cracks gradually widened and deepened, and many new irregular cracks appeared. After 1 h, the specimen began to collapse from the edge to the center and gradually became broken.

The initial color of rock specimen N-46 was earthen yellow, and its surface was relatively smooth. According to Fig. 4, powder fell off at the edge of the rock specimen and bubbles were generated when water was added. A long and wide crack appeared on the surface of the rock specimen accompanied by large bubbles. In a very short time, the crack extended to the edge, and a large amount of material fell directly along the crack to the bottom of the beaker.

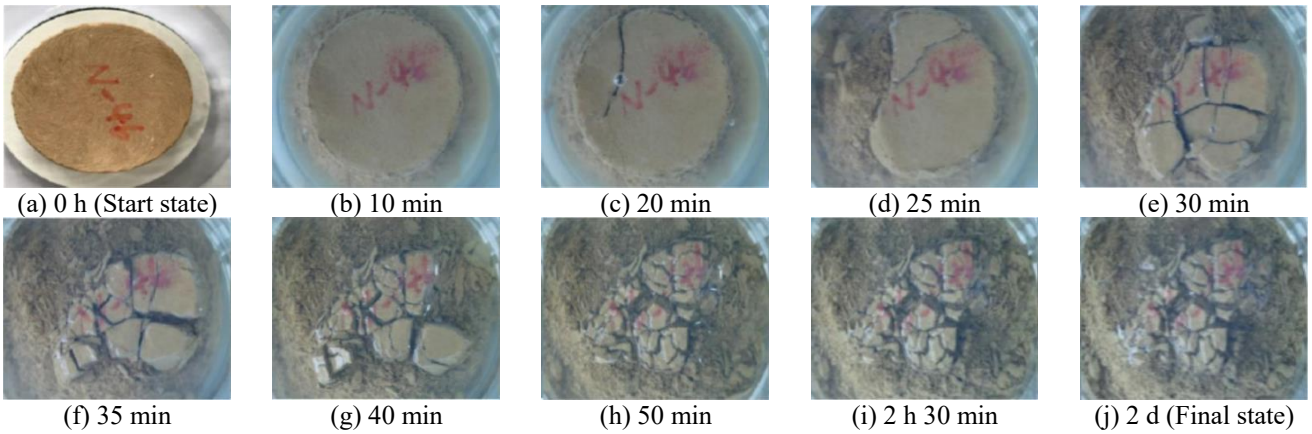

(a) 0 h (Start state) (b) 10 min (c) 20 min (d) 25 min (e) 30 min

(f) 35 min (g) 40 min (h) 50 min (i) 2 h 30 min (j) 2 d (Final state)

Fig. 4 Disintegration process of N-46

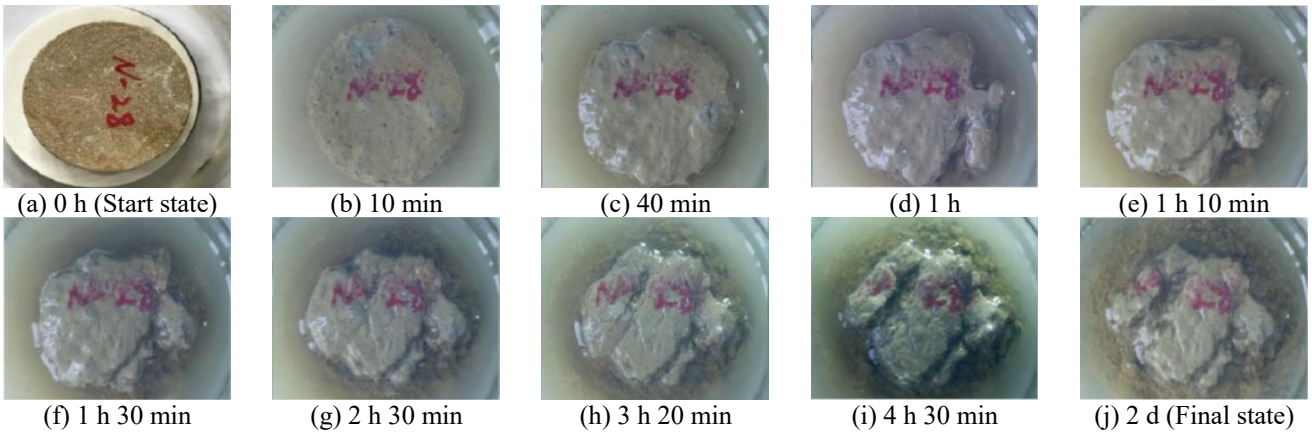

(a) 0 h (Start state) (b) 10 min (c) 40 min (d) 1 h (e) 1 h 10 min

(f) 1 h 30 min (g) 2 h 30 min (h) 3 h 20 min (i) 4 h 30 min (j) 2 d (Final state)

Fig. 5 Disintegration process of N-28

After 30 min, several deep, staggered cracks appeared in the specimen, dividing it into chunks. As the experiment continued, more fine fractures appeared in the rock specimens, the primary fractures deepened, and the block edges tended to collapse. Within 5-10 minutes, the rock specimen became more fragmented, and its integrity was almost destroyed. After a while the lower right block split and fell. The rock specimen basically had no obvious variation after 2 h 30 min, indicating that the expansion of N-46 specimen was completed in a short time, and the fracture development and block collapse speed were very fast.

The initial color of rock specimen N-28 was brownish gray, and the surface was smooth and filled with many fine debris particles. According to Fig. 5, when water was added, a small part of the specimen dissolved first, and the edge of the rock specimen presented circular dissolution traces. The specimen then dissolved and fell from the edge of the specimen, and when the fissure deepened enough, the pieces with the edges removed fell to the bottom of the beaker. As time passed, the expansion changes continued and the rock specimen developed two broad and deep main fractures, which were accompanied by the collapse of small fragments along the edges. In the process of expansion, the relative integrity of the rock specimen was maintained to a certain extent, and finally tended to be stable.

The rock specimen N-56 had an initial color of earthen yellow, with many scratches on its surface and filling with clastic particles. According to Fig. 6, when water was added to the specimen expands, part of the powder at the edge of the rock specimen began to fall off, and there were traces of dissolution on the surface. Then, cracks of varying width appeared at the edges of the specimen surface, with prominent denudation-like marks at the edges and wider cracks at the sides. Along the edge of the existing fracture, some fragments began to peel, accompanied by bubbles, and there were similar pulverization marks on the side of the rock specimen. In approximately 40 minutes, the side of the rock specimen had become very broken, and the cracks on the surface widened and deepened. At approximately 1 h 40 min, the rock specimen as a whole had been broken. Some of the blocks that had been ripped off by the cracks had fallen to the bottom of the beaker, and the rock specimen was almost incomplete. The expansion of the rock specimen was completed in a relatively short time.

Obviously, the disintegration characteristics of mudstone and sandy mudstone are different. Mudstone specimens generally exhibit cracks on the surface after being immersed in water for 10 min, cracks continue to extend, and new irregular cracks appear as the disintegration experiment proceeds. After 2-4 h, as the crack develops, the pattern will collapse from all sides to the center and break into small pieces. The modes of collapse of sandy mudstones are quite different. When sandy

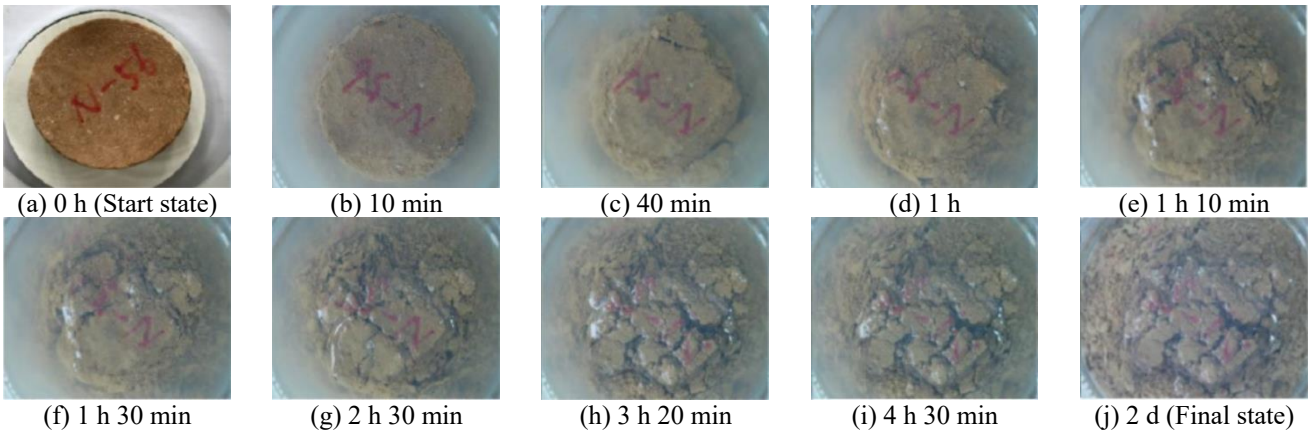

(a) 0 h (Start state) (b) 10 min (c) 40 min (d) 1 h (e) 1 h 10 min

(f) 1 h 30 min (g) 2 h 30 min (h) 3 h 20 min (i) 4 h 30 min (j) 2 d (Final state)

Fig. 6 Disintegration process of N-56

Table 4 Rock disintegration types and characteristics

Disintegration classification	Type of disintegration	Disintegration characteristics
I	Mud-like	Immersion in water instantly and violently disintegrates into earthy spills.
II	Broken gap mud, broken lump mud	Immersed in water into flocculent, powder crumbling, disintegrated material is granular, flaky broken gap or broken pieces.
III	Crushed rock chips, crushed rock pieces	Submerged in water into a block crumbling collapse or flake cracking, disintegrated material is broken rock flakes or broken rock-like.
IV	Integral block	Hard, non-disintegrating rock when immersed in water.

Table 3 Disintegration index of mudstone

Specimen type	Specimen number	I_d (%)	Average I_d (%)
Mudstone	N-6	0.1	0.1
	N-19	0.1	
	N-46	——	
Sandy mudstone	N-28	9.7	8.7
	N-62	7.7	

mudstone is immersed in water, water quickly seeps into the rock mass and bubbles are expelled. Within 1 h, the specimen expands continuously, cracks appear at the edges, and then gradually dissolves from the outside to the inside.

The air inside the specimen is squeezed inward and compressed with the entry of external water. The increase in air pressure in the specimen results in the gradual disintegration of minerals along the weakest plane of the structure (Arman *et al.* 2021, Ferraz *et al*. 2019).

From the actual observation, it can be concluded that the whole process of flooding disintegration of mudstone can be divided into three stages. In the first stage, after contact with water, surface particles adsorb water molecules, and the water film thickens. The soluble material dissolves and the structural connections on the rock surface are locally broken and disintegrate into small pieces. In the second stage, under the further action of water, microcracks develop to depth. With the disintegration of the clastic particles, the small pieces fall apart. The third stage is the dissolution of granular cements.

3.2 Disintegration index

Four specimens are taken from mudstone and sandy mudstone to calculate their I_d, respectively. After two wet-dry cycles, the specimens were sieved with a 2 mm aperture sieve. The mass of particles larger than 2 mm was recorded and I_d was calculated. The test results are shown in Table 3.

As seen from the data in Table 3, the disintegration resistance of mudstones generally deviated. According to the disintegration type and characteristics of mudstone, it can be divided into four disintegration grades I, II, III and IV. Grade I represent the weakest disintegration resistance, and grade IV represents the strongest disintegration resistance (Gautam and Shakoor 2017). The specific classification method is shown in Table 4.

From the calculation results and observation, it can be concluded that mudstone mainly belongs to grade III disintegration, and the disintegration type is broken rock. Sandy mudstone mainly belongs to grade II disintegration, the disintegration type is lump mud, and the disintegration speed is faster than mudstone (Chen *et al*. 2020).

3.3 Micro mechanisms of mudstone disintegration

3.3.1 Effects of clay minerals

Since the content of clay minerals tends to affect the water absorption of rocks, the difference in disintegration between specimens may also be related to it. Fig. 7 shows the clay mineral content and I_d of several classic disintegrating specimens.

As shown in Fig. 7, N-6, N-19 and N-46 are mudstones, while N-28 and N-56 are sandy mudstones. The results show that the content of clay minerals in mudstone is generally 25% higher than that in sandy mudstone, and the

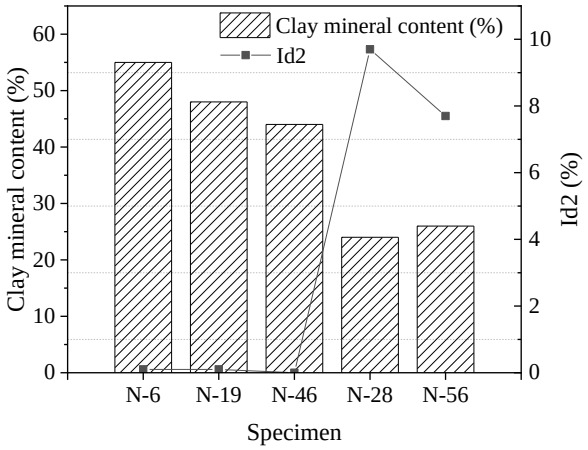

Fig. 7 Mudstone clay mineral content and I_d

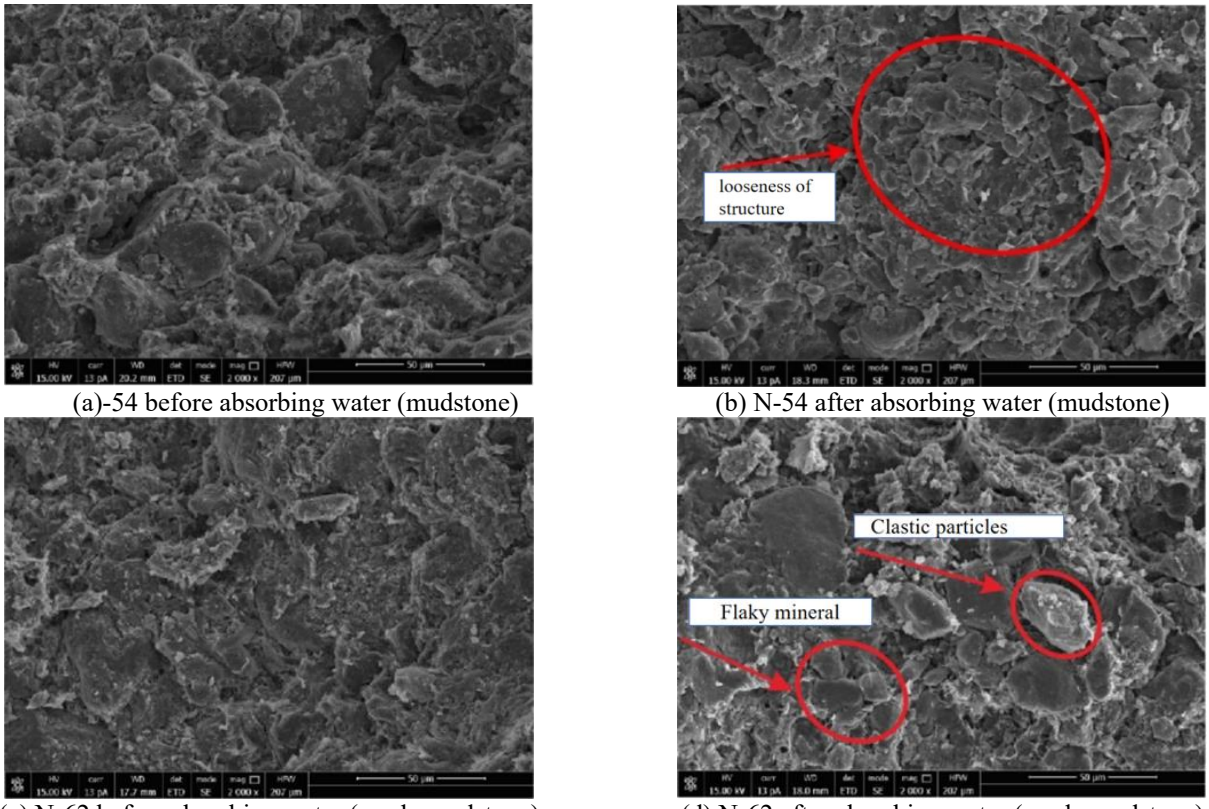

(a)-54 before absorbing water (mudstone) (b) N-54 after absorbing water (mudstone)

(c) N-62 before absorbing water (sandy mudstone) (d) N-62 after absorbing water (sandy mudstone)

Fig. 8 SEM image of mudstone and sandy mudstone before and after water absorption (Feng *et al.* 2022)

I_d of the corresponding mudstone is also 8.7% lower than that in sandy mudstone. The difference in clay content is indeed the cause of the difference in disintegration characteristics of mudstone. The mudstones with high clay mineral contents in Xining, China, are mainly stratified units (Nakano and Sakai 2016).

When water enters, a large number of cracks develop in the mudstone, causing the mudstone to collapse into blocks. The content of clay minerals in sandy mudstone is low, and the unit types are mostly clastic. After water enters the pores, most particles dissolve into the water due to the presence of clastic particle units, and eventually disintegrate into mud (Chen *et al*. 2018).

Fig. 8 shows SEM images of mudstone and sandy mudstone before and after water absorption, respectively (Feng *et al.* 2022). As shown in Fig. 9, after mudstone absorbs water, its overall structure changes from dense to lose, pore size increases, the number of pores increases, and the clay minerals change into a state of layer separation. Sandy mudstone is relatively complete in structure and the volume of clay minerals expands (Kim *et al*. 2018). The physical changes of mudstone specimens after water absorption during the experiment can be divided into two parts. On the one hand, the vacancy in the pore and pore

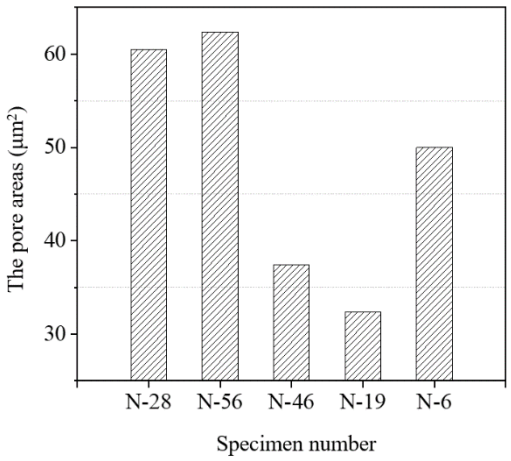

Fig. 9 Pore area of different specimens

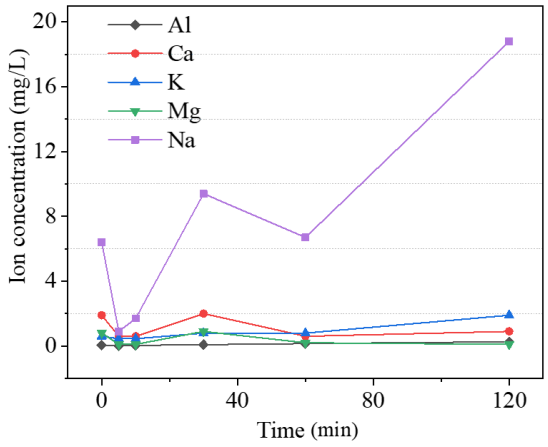

Fig. 10 Changes in concentration of cations in aqueous solution

boundary will cause the pore to become larger. On the other hand, with the expansion of mineral volume, pores and fissures are gradually squeezed, resulting in the reduction of fissures and pores between mudstone minerals. With the expansion of schistose minerals, the water absorbing film thickens. This leads to an increase in spacing, resulting in separation between layers, which in turn destroys the entire structure (Waroszewski *et al.* 2015).

3.3.2 Effect of pore structure

The effect of pore structure on disintegration is also important. Image Pro Plus (IPP) image analysis software was used to study the pore characteristics of mudstone specimen pairs. Fig. 9 shows the pore areas of several observed specimens. The larger the pore area is, the stronger the disintegration of mudstone. When the pore area is large, water will enter the pore rapidly in a short time, causing a large amount of soluble salt to dissolve. The air in the rock is squeezed into internal compression, and the internal air pressure increases rapidly, leading to the fracture of minerals along the most vulnerable structural plane. Then the mudstone directly disintegrates into mud.

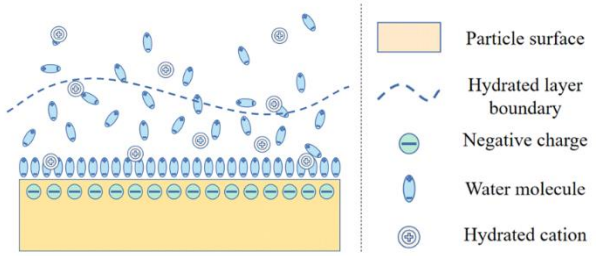

Fig. 11 Hydration reaction on the kaolinite particle surface (Zeng *et al.* 2021)

3.3.3 Disintegration mechanism

The disintegration test results show that the disintegration process of sandy mudstone is rapid and intense, and specimen N-56 is the most representative specimens. The chemical change of the N-56 specimen was studied by extracting the solution during disintegration. Its ionic composition was measured at regular intervals, and the experimental results are shown in Fig. 10. In this part, the ionic composition was analyzed through Atomic Absorption Spectroscopy (AAS) method.

The contents of Na and Ca ions in aqueous solutions of mudstone are higher. Except for Na and K ions, the concentrations of Al, Ca and Mg ions did not change significantly. Ion exchange occurred on the mudstone surface within 1 hour, and the ion solubility fluctuated in a small range. The mudstone structure is relatively intact at this time. After 1 hour, a large amount of soluble salt dissolved, the concentration of Na and K ions increased, and the structure of mudstone was damaged. The results are consistent with the mudstone disintegration test, so the disintegration of mudstone is related to the loss of salt inside the rock.

Table 1 shows that the mudstone is also rich in kaolinite minerals. Kaolinite is mainly connected by oxygen–oxygen bonds to its microscopic units. When a mudstone specimen is immersed in water, water molecules can easily enter the specimen through the primary cracks. The oxygen–oxygen bond, which is inherently less stable, will break. As shown in Fig. 11, aluminum ions (Al^{3+}) in the structural unit often exchange with some low-valence cations (Mg^{2+} etc.), resulting in many negative charges on the surface of the structural unit. The cations in the water are then adsorbed to the surface and become hydrated cations (H_3O^+). When the hydrated cation slowly infiltrates between the structural unit and the hydrated layer, the distance between the layers and the thickness will increase, and then the spectator particles will expand. Because the inside and outside sides of the specimen cannot absorb water at the same time, it will lead to uneven expansion of the particle surface. This may result in tensile stress on the surface, causing further damage to the already fractured rock surface (Chen *et al.* 2019). Part of the chemical reaction equation is as follows.

$$K_2[AlSi_3O_8](\text{K-Feldspar})+H_2O \rightarrow K^+ + KAl_2[(Si,Al)_4O_{10}][OH]_2 \ (\text{Illite}) \quad (2)$$

$$Na_2[AlSi_3O_8](\text{Na-Feldspar})+H_2O \rightarrow Na^+ + 2NaAl_2[(Si,Al)_4O_{10}][OH]_2 \ (\text{Montmorillonite}) \quad (3)$$

$$Al_4[Si_4O_{10}][OH]_8(\text{Kaolinite})+H_2O+CO_2 \rightarrow Al^{3+}+H_4SiO_4+HCO_3^- \quad (4)$$

$$KAl_2[(Si,Al)_4O_{10}][OH]_2(\text{Illite})+H_2O+CO_2 \rightarrow K^++Al^{3+}+H_4SiO_4+HCO_3^- \quad (5)$$

4. Conclusions

This paper takes mudstone in the Xining area as the research object. They are divided into two types based on the microstructure, and then the disintegration process of several typical specimens is observed. Finally, the disintegration mechanism is analyzed from three aspects: clay minerals, ion exchange and energy transformation. The main conclusions are as follows.

• In the disintegration test, the two kinds of mudstones both collapse quickly in the early stage and tend to be stable in the later stage. The mudstone cracks in approximately ten minutes and develops over the next hour, creating new irregular cracks and finally breaking into blocks. The main disintegration of sandy mudstone is mud, disintegration is dissolved from the surroundings while producing bubbles, and disintegration is basically completed in approximately 1 h.

• The clay content of mudstone is approximately 25% higher than that of sandy mudstone, and the pore area is approximately 20 μm^2 larger than that of sandy mudstone. These two factors affect the microstructure of the mudstone and are negatively correlated with disintegration, making the disintegration rate of the sandy mudstone slightly faster.

• By analyzing the variation trend of the chemical composition of the water solution in the disintegration test, it is concluded that the ions in the mudstone specimen are exchanged and combined with each other by water molecules in the environment during the whole disintegration process. These chemical changes lead to the continuous spalling and splitting of clay minerals in the two mudstone specimens, the emergence of secondary fractures, and the deepening of primary fractures until disintegration.

Competing interests

The authors declare that they have no competing interests.

Acknowledgements

We would like to thank Analytical and Testing Center of Southwest Jiaotong University. The research presented here is supported by the National Key Research and Development Program of China (2023YFC3707801), National Natural Science Foundation of China (52078317), Natural Science Foundation of Jiangsu Province for Excellent Young Scholars (BK20211597), project from Bureau of Housing and Urban-Rural Development of Suzhou (2021-25; 2021ZD02; 2021ZD30; 2023ZD26), Bureau of Geology and Mineral Exploration of Jiangsu (2021KY06), China Tiesiju Civil Engineering Group (2021-19), and CCCC Tunnel Engineering Company Limited (8gs-2021-04)..

References

Aksoy, M., Ankara, H. and Kandemir, S.Y. (2019), "Preparation and evaluation of spherical samples for Slake Durability Index test", *Int. J. Environ. Sci. Technol.*, **16**(9), 5243-5250. https://doi.org/10.1007/s13762-019-02254-1.

Arman, H., Abdelghany, O., Saima, M.A., Aldahan, A., Paramban, S. (2021), "Slaking behavior of evaporitic rocks from Abu Dhabi area, United Arab Emirates", *Arabian J. Geosci.*, **14**(11), 1-8. https://doi.org/10.1007/s12517-021-07295-w.

ASTM D4644-08. (2008), Standard Test Method for Slake Durability of Shales and Similar Weak Rocks. West Conshohocken, PA: ASTM International.

Boulesteix, K., Poyatos-Moré, M., Hodgson, D.M., Flint, S. and Taylor, K.G. (2020), "Fringe or background: Characterizing deep-water mudstones beyond the basin-floor fan sandstone pinchout", *J. Sediment. Res.*, **90**(12), 1678-1705. https://doi.org/10.2110/jsr.2020.048.

Chen, J.N., Salihoglu, H., Benson, C.H. and Likos, W.J. (2019), "Hydraulic conductivity of bentonite-polymer geosynthetic clay liners to coal combustion product leachates", *J. Geotech. Geoenviron. Eng.*, **145**(9). https://doi.org/10.1007/978-981-13-2224-2_82.

Chen, J.N., Tinjum, J. and Edil, T. (2013), "Leaching of alkaline substances and heavy metals from recycled concrete aggregate used as unbound base course", *Transp. Res. Rec.*, (2349), 81-90. https://doi.org/10.3141/2349-10.

Chen, J.N., Ren, X., Xu, H. and Zhang, C. (2022), "Effect of grain size and moisture content on the interfacial shear behavior between sandy soil and geogrid", *Int. J. Geomech.*, accepted.

Chen, J.N., Benson, C.H. and Edil, T.B. (2018), "Hydraulic conductivity of geosynthetic clay liners with sodium bentonite to coal combustion product leachates", *J. Geotech. Geoenviron. Eng.*, **144**(3). https://doi.org/10.1061/(ASCE)GT.19435606.0001844.

Chen, J.N., Sanger, M., Ritchey, R., Ginder-vogol, M. and Edil, T.B. (2020), "Neutralization of high pH and alkalinity effluent from Recycled Concrete Aggregate (RCA) by common subgrade soil", *J. Environ. Qual.*, **49**(1), 172-183. https://doi.org/10.1002/jeq2.20008.

DeReuil, A.A., Birgenheier, L.P. and McLennan, J. (2019), "Effects of anisotropy and saturation on geomechanical behavior of mudstone", *J. Geophys. Res.: Solid Earth*, **124**(8), 8101-8126. https://doi.org/10.1029/2018JB017034.

Dner, Z., Hu, Q., Kumral, M., Kibria, M.G. and Sun, M. (2021), "Petrophysical characteristics of silurian mudstones from central taurides in Southern Turkey", *J. Earth Sci.*, **32**(4), 778-798. https://doi.org/10.1007/s12583-021-1408-0.

Dupontnivet, G., Hoorn, C. and Konert, M. (2008), "Tibetan uplift prior to the Eocene-Oligocene climate transition: Evidence from pollen analysis of the Xining Basin", *Geol.*, **37**(6), 987. https://doi.org/10.1130/0091-7613-37.6.506.

Feng, Z., Xu, Q., Luo, X., Huang, R., Liao, X. and Tang, Q. (2022), "Microstructure, deformation characteristics and energy analysis of mudstone under water absorption process", *Energies*, **15**(20), 7511. https://doi.org/10.3390/en15207511.

Ferraz, E. and Gamelas, J., Coroado, J., Monteiro, C. and Rocha, F. (2019), "Recycling waste seashells to produce calcitic lime: Characterization and wet slaking reactivity", *Waste Biomass Valorization*, **10**(8), 2397-2414. https://doi.org/10.1007/s12649-018-0232-y.

Gautam, T.P. and Shakoor, A. (2019), "A durability classification of clay-bearing rocks based on particle size distribution of slaked material", *Environ. Eng. Geosci.*, **23**(2), 125-135. https://doi.org/10.2113/gseegeosci.23.2.125.

Gautam, T.P. and Shakoor, A. (2016), "Comparing the slaking of clay-bearing rocks under laboratory conditions to slaking under natural climatic conditions", *Rock Mech. Rock Eng.*, **49**(1), 19-31. https://doi.org/10.1007/s00603-015-0729-7.

Gautam, T.P. and Shakoor, A. (2013), "Slaking behavior of clay-bearing rocks during a one-year exposure to natural climatic conditions", *Eng. Geol.*, **166**(8), 17-25. https://doi.org/10.1016/j.enggeo.2013.08.003.

Iyare, U.C., Blake, O.O. and Ramsook, R. (2021), "Modelling the failure behavior of mudstones under high pressures", *Rock Mech. Rock Eng.*, 1-14. https://doi.org/10.1007/s00603-021-02467-2.

Kim, E., Garcia, A. and Changani, H. (2018), "Fragmentation and energy absorption characteristics of Red, Berea and Buff sandstones based on different loading rates and water contents", *Geomech. Eng.*, **4**(2), 151-159. https://doi.org/10.12989/gae.2018.14.2.000.

Kim, J.Y., Park, Y.H. and Cho, K.H. (2018), "Study on applicability of shale as an embankment material in railway roadbed using slake durability test", *J. Korean Soc. railway*, **21**(2), 166-176. https://doi.org/10.7782/JKSR.2018.21.2.166.

Koralegedara, N.H. and Maynard, J.B. (2017), "Chemical, mineralogical and textural properties of the Kope Formation mudstones: How they affect its durability", *Eng. Geol.*, **228**: 312-322. https://doi.org/10.1016/j.enggeo.2017.08.025.

Luo, X., Gao, H., He, P. and Liu, W. (2021), "Experimental investigation of dry density, initial moisture content, and temperature for granite residual soil disintegration", *Arabian J. Geosci.*, **14**(11). https://doi.org/10.1007/s12517-021-07239-4.

Meisels, R., Toifl, M., Hartlieb, P., Kuchar, F. and Antretter, T. (2015), "Microwave propagation and absorption and its thermo-mechanical consequences in heterogeneous rocks", *Int. J. Min. Process.*, **135**: 40-51. https://doi.org/10.1016/j.minpro.2015.01.003.

Milroy, P., Wright, V.P. and Simms, M.J. (2019), "Dryland continental mudstones: Deciphering environmental changes in problematic mudstones from the Upper Triassic (Carnian to Norian) Mercia Mudstone Group, south-west Britain", *Sedimentology*, **66**(7). https://doi.org/10.1111/sed.12626.

Momeni, A., Hashemi, S.S., Khanlari, G.R. and Heidari, M. (2017), "The effect of weathering on durability and deformability properties of granitoid rocks", *Bull. Eng. Geol. Environ.*, **76**(3), 1-13. https://doi.org/10.1007/s10064-016-0999-7.

Mori, M., Sakagami, Y., Hamazaki, Y. and Jojima, T. (2018), "Evaluation of the influence of sprinkling powdered slaked lime on microorganisms for the prevention of domestic animal infectious diseases", *Environ. Technol.*, 1-40. https://doi.org/10.1080/09593330.2018.1465128.

Nakano, M. and Sakai, T. (2016), "Interpretation of slaking of a mudstone embankment using soil skeleton structure model concept and reproduction of embankment failure by seismic analysis", *Japanese Geotechnical Society Special Publication*, **2**(5), 282-287. https://doi.org/10.3208/jgssp.JPN-124.

Park, S.S., Ye, S.R. and Kim, G.W. (2016), "Slaking characteristics of shale in the Gyoungsang Super-group, Korea", *J. Eng. Geol.*, **26**(3), 315-324. https://doi.org/10.9720/kseg.2016.3.315.

Pesce, C., Pesce, G.L., Molinari, M. and Richardson, A. (2020), "Effects of organic additives on calcium hydroxide crystallisation during lime slaking", *Cement. Concrete Res.*, **139**, 106254. https://doi.org/10.1016/j.cemconres.2020.106254.

Sakai, T. and Nakano, M. (2015), "Interpretation of the mechanical behavior of embankments having various compaction properties based on the soil skeleton structure – ScienceDirect", *Soils Found.*, **55**(5), 1069-1085. https://doi.org/10.1016/j.sandf.2015.09.009.

Sargent, C., Andras, P., Goulty, N.R. and Aplin A.C. (2016), "Compaction of diagenetically altered mudstones - Part 1: Mechanical and chemical contributions", *Mar. Pet. Geol.*, **77**: 703-713. https://doi.org/10.1016/j.marpetgeo.2016.07.015.

Selen, L., Panthi, K.K. and Vistnes, G. (2019), "An analysis on the slaking and disintegration extent of weak rock mass of the water tunnels for hydropower project using modified slake durability test", *Bull. Eng. Geol. Environ.*, **79**(4). https://doi.org/10.1007/s10064-019-01656-2.

Shakoor, A. and Gautam, T.P. (2015), "Influence of geologic and index properties on disintegration behavior of clay-bearing rocks", *Environ. Eng. Geosci.*, **21**(3), 197-209. https://doi.org/10.2113/gseegeosci.21.3.197.

Shumilova, T.G., Shevchuk, S.S. and Isayenko S.I. (2016), "Metal concentrations and carbonaceous matter in the black shale type rocks of the Urals", *Doklady Earth Sciences*, **469**(1), 695-698. https://doi.org/10.1134/S1028334X16070060.

Tang, Q., Gu, F., Zhang, Y., Zhang, Y.Q. and Mo, J.L. (2018), "Impact of biological clogging on the barrier performance of landfill liners", *J. Environ. Manage.*, **222**, 44-53. https://doi.org/10.1016/j.jenvman.2018.05.039.

Tang, Q., Katsumi, T., Inui, T. and Li, Z.Z. (2014), "Membrane behavior of bentonite amended compacted clay", *Soils Found.*, **54**(3), 329-344. https://doi.org/10.1016/j.sandf.2014.04.019.

Tang Q., Katsumi T., Inui T., Li Z.Z. (2015), "Influence of pH on the membrane behavior of bentonite amended Fukakusa clay", *Sep. Purif. Technol.*, **141**, 132-142. https://doi.org/10.1016/j.seppur.2014.11.035.

Tang, Q., Zhang, Y., Gao, Y.F. and Gu, F. (2017), "Use of cement-chelated solidified MSWI fly ash for pavement material: mechanical and environmental evaluations", *Can. Geotech. J.*, **54**(11), 1553-1566. https://doi.org/10.1139/cgj-2017-0007.

Vu, H.H.T., Gu, S., Thriveni, T., Khan, M.D., Lai, Q.T. and Ji, W.A. (2019), "Sustainable treatment for sulfate and lead removal from battery wastewater", *Sustainability*, **11**(13), 3497. https://doi.org/10.3390/su11133497.

Waroszewski, J., Kabala, C. and Jezierski, P. (2015), "Relief-induced soil differentiation at the sandstone-mudstone contact in the Stołowe Mountains, SW Poland", *Zeitschrift Für Geomorphologie*, **59**(1), 211-226. https://doi.org/10.1127/zfg_suppl/2015/S-00181.

Yin, H.W., Ma, H.L., Chen, X.S., Shi, X., Yang, C., Maurice, D. and Zhang, Y. (2017), "Synthetic rock analogue for permeability studies of rock salt with mudstone", *Appl. Sci.*, **7**(9). https://doi.org/ 10.3390/app7090946.

Zhang, L., Mao, X., Li, M., Li, B., Liu, R. and Lu, A. (2020), "Brittle–ductile transition of mudstone in coal measure rock strata under high temperature", *Int. J. Geomech.*, **20**(1). https://doi.org/10.1061/(ASCE)GM.19435622.0001549.

Zdemr, S. and Ergler, Z.A. (2021), "Investigation of the slaking behavior of weak geological units in terms of undercutting rate", *Bull. Min. Res. Explor.*, **167**, 111-125. https://doi.org/10.19111/bulletinofmre.898013.

Zeng, L., Luo, J.T., Liu, J. and Gao, Q.F. (2021), "Disintegration characteristics and mechanisms of carbonaceous mudstone subjected to load and cyclic drying–wetting", *J. Mater. Civ. Eng.*, **33**(8), 04021195. https://doi.org/10.1061/(ASCE)MT.1943-5533.0003817

CC